SOLAR-WIND ENERGY INTEGRATION IN THE NIGERIAN 330 kV GRID: A TECHNICAL ANALYSIS

Ugwoke, N. C.[1*], Ugwuanyi, N. S.[2], Ezeonye, C. S.[3], Onwuka, I. K.[1], Obi, P. I.[1], Onah, A. J.[1]

[1] Department of Electrical & Electronic Engineering, Michael Okpara University of Agriculture, Umudike, Abia State
[2]Department of Electrical & Electronics Engineering, Alex Ekwueme Federal University, Ndufu-Alike, Ebonyi State
[3]Department of Electrical & Electronic Engineering, University of Agriculture and Environmental Sciences, Umuagwo, Imo State
Email: [1*]nestorchima202@gmail.com, [2]ugwuanyi.nnaemeka@funai.edu.ng, [3]ezeonyechinonso@yahoo.com, [1]onwuka.ifeanyichukwu@mouau.edu.ng, [1]patndyobi@gmail.com, [1]aniagbosoonah@yahoo.com

ABSTRACT
This paper conducts a detailed technical analysis of the integration of solar and wind energy into Nigeria's 330 kV power grid. Despite extensive power sector reforms, Nigeria's energy demand continues to surpass supply, with heavy reliance on fossil fuels leading to an unreliable and unsustainable power system. Given the country's substantial wind and solar energy potential, this study examines the impact of incorporating these renewable sources on grid stability and active power loss. Using the Power System Analysis Toolbox (PSAT) in MATLAB, the study models Nigeria's 50-bus, 330 kV grid, and includes case studies comparing scenarios with different levels of renewable energy penetration. The findings indicate that the integration of wind and solar energy enhances system stability and increases renewable energy penetration limits, particularly when both energy sources are combined. Active power losses decrease significantly when penetration rates are optimized, with wind energy allowing for a 15% penetration limit and a combined wind-solar configuration reaching up to 25%. Furthermore, the study identifies significant improvements in small-signal stability, with damping ratios and eigenvalues improving with higher renewable penetration. This analysis underscores the feasibility of renewable energy integration as a solution for Nigeria's energy challenges, contributing to cleaner, more reliable electricity generation.

Keywords: Doubly-Fed Induction Generator, Nigerian 330 kV Grid, Power System Stability, Renewable Energy Integration, Solar Photovoltaic.

1.0 INTRODUCTION
Despite power sector reforms in Nigeria, many citizens still lack access to electricity. There remains a significant gap between electricity demand and supply, with overreliance on fossil fuels and minimal hydro contributions (Chukwulobe *et al*., 2022). Population growth and increasing energy demand, combined with unsustainable fossil fuel generation due to climate change (Obi *et al*., 2021; Emeasoba *et al*., 2023), have worsened the situation. Factors such as outdated transmission and distribution equipment, insufficient power plants, poor metering, underfunding, vandalism, technical losses, and corruption contribute to the unreliable power sector (Obi *et al*., 2022). To address these issues, researchers have focused on integrating renewable energy, especially solar and wind, as cleaner alternatives. Some argue that 100% renewable energy integration is unattainable due to transmission limitations (Brown *et al*., 2018), while others claim it is feasible (Narayanan *et al*., 2019). Countries like Iceland (100%), Paraguay (99%), and Norway (97%) have made significant progress (Zappa *et al*., 2019).
Globally, wind energy is rapidly growing, with over 591 GW of installed capacity (Chau, 2019; Adetokun *et al*., 2020). Wind energy, abundant in Nigeria (Okeniyi *et al*., 2015; Somoye, 2023; Okedu *et al*., 2024), varies by region, with the North-West having the highest wind speeds ranging from 3.88 – 9.39m/s (Oluleye and Debo, 2016). However, some report lower wind speeds within the range of 1.4 – 3.0m/s (Shaaban and Petinrin, 2014; Mas'ud *et al*., 2015), while others suggest higher figures of 8m/s at 50m height in northern regions (Akuru *et al*., 2017). Solar PV, another fast-growing renewable energy source, has proven reliable in developed nations (Ohunakin *et al*., 2014). Globally, cumulative solar PV capacity reached 627 GW in 2019 (REN21, 2020). In Nigeria, solar energy systems remain underdeveloped, limited to small-scale uses like

household and street lighting with only 15 MW of solar PV installed nationwide (Sambo, 2009). Some researchers argue that solar integration improves voltage stability (Adetokun *et al*., 2021), though others claim it affects damping ratios instead (Srivastava *et al*., 2018).

Adedipe *et al*. (2018) note that despite Nigeria's significant wind and solar energy potential, these resources currently make no contribution to the national grid. Small-scale wind turbines are mainly used for non-grid purposes, with limited capacity installations in Sokoto and Kastina states (Akuru *et al*., 2017; Mohammed *et al*., 2017). Studies on small signal stability show conflicting results, with some finding that wind energy integration improves damping (Ayodele *et al*., 2013; Yang *et al*., 2013), while others argue that it reduces the damping ratio (Berrutti *et al*., 2012; Essallah *et al*., 2019). Similarly, voltage stability analyses show that wind energy's impact varies depending on location and control methods (Bekri and Mekri, 2018; Naser *et al*., 2021; Atta *et al*., 2022). In Nigeria, studies using permanent magnet synchronous-based wind turbines show improved voltage profiles (Olanrewaju *et al*., 2022), while increasing power injection from wind plants enhances voltage margin and loadability (Adetokun *et al*., 2020; Krismanto *et al*., 2021). However, loadability decreases with higher wind penetration (Gurung *et al*., 2020). The interaction between wind and conventional plants also presents new stability challenges (Qin *et al*., 2020; Tavakoli *et al*., 2020). In Nigeria, Doubly-fed induction generator (DFIG)-connected systems improve penetration when connected via load buses rather than replacing existing generators (Ozioko *et al*., 2022). FACTS devices have been proposed to improve power system stability with wind integration. Studies show that devices like STATCOM and UPFC enhance voltage stability, extend penetration limits, and reduce power losses (Nkan *et al*., 2019; Dhouib *et al*., 2020; Ugwuanyi *et al*., 2024a; Ugwuanyi *et al*., 2024c). Many researchers agree that optimal placement of FACTS devices increases stability and loadability (Anichebe and Ekwue, 2020; Offiong *et al*., 2022; Ogunbiyi *et al*., 2022).

Building on previous research, this paper investigates the concurrent integration of wind and solar energy, into the Nigerian grid, providing a comprehensive analysis of this multi-source approach. The technical investigation centers on two critical parameters stability (small- and large-signal) and active power loss, which are vital to ensuring reliable power system operation.

2.0 THEORETICAL BACKGROUND OF RENEWABLE ENERGY INTEGRATION

This section provides a comprehensive review of the theoretical foundations of renewable energy integration, essential for understanding the principles and challenges associated with incorporating wind and solar power into the grid.

2.1 Dynamic Modelling of Wind Turbine

A modern wind turbine consists of four key components: the tower, nacelle, yaw mechanism, and rotor. These components synergistically convert wind energy into electrical energy. In load flow studies, wind energy integration is modelled using various approaches, including real-reactive power (PQ), real power-voltage (PV), and resistance-reactance (RX)-controlled models (Feijo and Cidrass, 2000). This paper concentrates on the PQ model, which is particularly well-suited for power factor control and facilitates the analysis of wind energy integration into the grid.

Figure 1 is a schematic representation of doubly-fed induction generator (DFIG) connected to the grid. The wind turbine model basically represents the relation between the mechanical power (Emeghara *et al*., 2022) extracted from the turbine $P_{wind\ and}$ the wind speed as

$$P_{wind} = \frac{1}{2}\rho A_{wt} C_p(\lambda, \theta) v_{wind}^3, \quad (1)$$

where ρ *i*s the air density, $A_{wt}$is the wind turbine swept area, v_{wind} is the wind speed, $C_p$is the power coefficient, λ is the tip speed, θ is the pitch angle.

Considering a fixed pitch angle, typical power curves are function of the wind speed and the electrical rotor speed. Also, considering manufacturer data and optimization techniques, a power coefficient function has been derived for a variable speed wind turbine. The DFIG model includes simplified turbine aerodynamics,

drive-train, shaft, generator, and converter. As a wound rotor induction machine, both stator and rotor participate in energy conversion, as illustrated in the equivalent circuit on Figure 2.

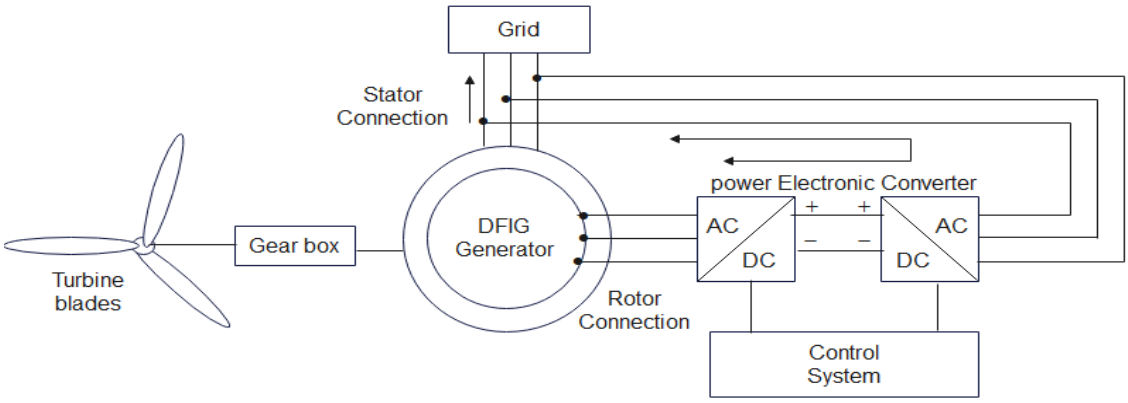

Figure 1: Schematic representation of doubly-fed induction generator (DFIG)

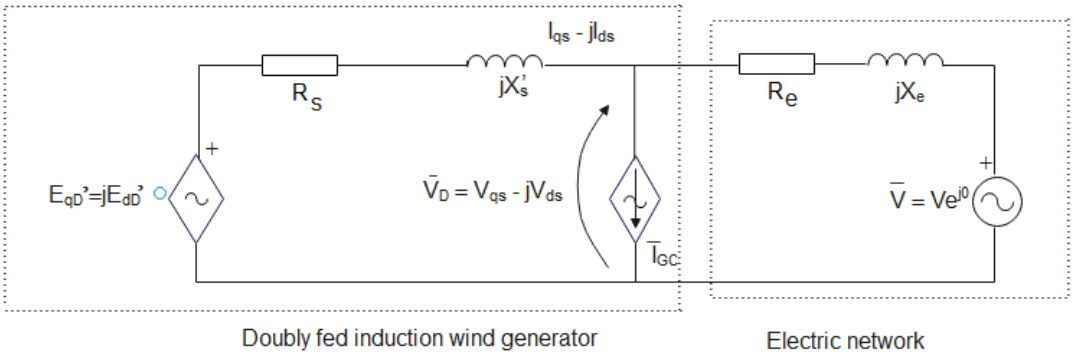

Figure 2: Equivalent circuit of a doubly fed induction generator connected to a grid

The stator, rotor circuits, and rotatory mass equation of motion yield the following differential equations as stated in (Ukoima *et al*., 2019; Emeghara *et al*., 2022)

$$\frac{1}{\omega_s}\frac{d\psi_{qs}}{dt} = V_{qs} + R_s I_{qs} - \psi_{ds} \quad (2)$$

$$\frac{1}{\omega_s}\frac{d\psi_{ds}}{dt} = V_{ds} + R_s I_{ds} + \psi_{qs} \quad (3)$$

$$\frac{1}{\omega_s}\frac{d\psi_{ds}}{dt} = V_{qr} - R_r I_{qr} - \left(\frac{\omega_s - \omega_r}{\omega_s}\right)\psi_{ds} \quad (4)$$

$$\frac{1}{\omega_s}\frac{d\psi_{dr}}{dt} = V_{dr} - R_r I_{dr} + \left(\frac{\omega_s - \omega_r}{\omega_s}\right)\psi_{qr}, \quad (5)$$

$$2\frac{H_D}{\omega_s}\frac{d\omega_r}{dt} = T_m - T_e, \quad (6)$$

where the system variables are defined as follows
R_r, R_s: rotor and stator resistance
ψ_{ds}, ψ_{qs}, ψ_{dr}, ψ_{qr}: stator and rotor *d*-axis and *q*-axis flux linkages
T_e: electrical torque
T_m: mechanical torque (wind velocity-dependent)
ω_s: synchronous speed (pu)
ω_r: rotor electrical speed
V_{ds}, V_{qs}, V_{dr}, V_{qr}: stator and rotor *d*-axis and *q*-axis voltages
I_{ds}, I_{qs}, I_{dr}, I_{qr}: stator and rotor *d*-axis and *q*-axis currents
H_D: generator inertia

The rotor flux equations are formulated using E'_{qD} and E'_{dD} as

$$I_{dr} = \frac{E'_{qD}}{X_m} + \frac{X_m}{X_r} I_{ds} \quad (7)$$

$$I_{qr} = -\frac{E'_{dD}}{X_m} + \frac{X_m}{X_r} I_{qs} \quad (8)$$

A phasor machine representation to calculate stator algebraic variables, given E'_{qD} and E'_{dD} is obtained.

$$E'_{qD} - E'_{dD} = (R_s + jX'_s)(I_{qs} - jI_{ds}) + V_{qs} - jV_{ds}, \quad (9)$$

where E'_{dD} and E'_{qD} are the equivalent *d*-axis and *q*-axis source voltage behind transient impedance respectively, X_m is mutual reactance, X_r is rotor reactance, X'_s is equivalent stator reactance.

2.2 Dynamic Modelling of Solar Photovoltaic Generator

Figure 3 depicts a grid-connected solar photovoltaic (SPV) system utilizing two-stage converters (DC-DC and DC-AC). In load flow studies, two primary models are employed: PQ-controlled and PV-controlled. The selection of model depends on the designer's goals. This study adopts the PV-controlled model, which enables voltage regulation and facilitates the analysis of voltage control objectives.

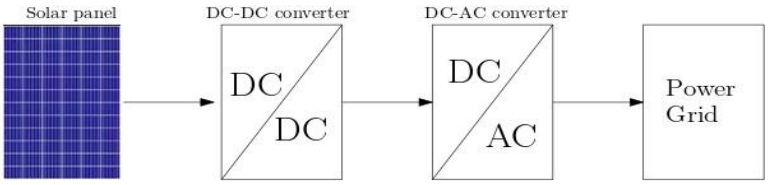

Figure 3: Schematic diagram of SPV connected to the grid

To facilitate analysis, this study focused on photovoltaic (PV) array's dynamics with a constant power load, assuming negligible resistive losses. The corresponding simplified circuit is shown in Figure 4.

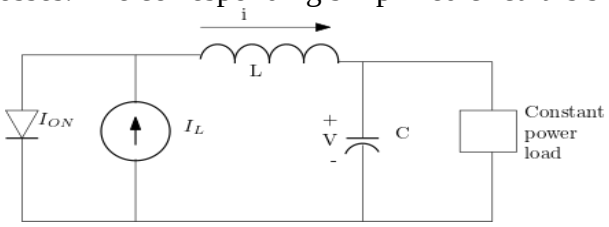

Figure 4: Simplified PV array with output elements

Kirchhoff's laws at both nodes yield

$$I_L - I_s\left\{exp\left[\alpha\left(v + L\frac{di}{dt}\right)\right] - 1\right\} - i = 0, \quad (10)$$

where I_s is the saturation current of the diode.

$$i - C\frac{dv}{dt} - \frac{p}{v} = 0 \quad (11)$$

where p is the constant power load.

Therefore, the dynamics of the systems are given by

$$\frac{di}{dt} = \frac{1}{L}\left[\frac{1}{\alpha} ln\left(\frac{I_L - i}{I_s} + 1\right) - v\right] \quad (12)$$

$$\frac{dv}{dt} = \frac{1}{C}\left[i - \frac{p}{v}\right] \quad (13)$$

where thermal diffusion, $\alpha = q/nskT$, $k = 1.3807 \times 10^{-23}$ JK^{-1} is Boltzmann's constant, $q = 1.6022 \times 10^{-19}$ C is the electronic charge, T = 298K is the temperature, *n* is electron density and *s* is surface recombination velocity.

2.3 Small Signal Stability Analysis

Power system dynamics can be modelled by the differential equation:

$$\dot{x} = f(x, u), \quad (14)$$

where x is a vector of state variables from Equations (2) – (6) and (12) – (13), while u is a vector of input variables. The linearization of Equation (14) gives

$$\Delta\dot{x} = A\Delta x + B\Delta u. \quad (15)$$

The eigenvalues can be complex or real or zero. For complex eigenvalues, it appears in the complex conjugate pair. A system is said to be stable in all operations if all the eigenvalues λ of A are at the left plane.

$$\lambda = \sigma \pm j\omega \quad (16)$$

The eigenvalues in power systems are usually referred to as oscillation modes. Therefore, the damping ratio, time constant and the frequency are given as

$$\varsigma = \frac{-\sigma}{\sqrt{\sigma^2+\omega^2}}. \quad (17)$$

$$f = \frac{\omega}{2\pi}, \quad (18)$$

where ς is the damping ratio, f is the frequency, ω is the angular frequency.

In this paper, 5% and above are taken to be sufficient in the power system analysis.

3.0 METHODOLOGY

This study employs modelling and simulation as its investigative methodology. Specifically, the Nigerian 330 kV power system is modeled using Power System Analysis Toolbox (PSAT) within a MATLAB environment.

3.1 Power System Analysis Toolbox (PSAT)

Power System Analysis Toolbox (PSAT) is a free, open-source, MATLAB-based software package for power system analysis and simulation. Developed by Federico Milano, PSAT offers a range of features including power flow, continuation power flow, small signal stability, transient stability, fault analysis, and optimal power flow. Suitable for power system planning, design, and research, PSAT provides a user-friendly interface, flexible modelling capabilities, and fast simulation times, making it an ideal tool for power engineers and researchers. PSAT features detailed models of DFIG and SPV systems, supporting PQ and PV control modes, to facilitate accurate simulations of renewable energy integration.

3.2 The Nigerian 50 – Bus, 330 kV Power System

Figure 5 presents a streamlined model of Nigeria's 50-bus power grid, which includes 14 generating stations (3 hydroelectric and 11 gas-powered plants) and a total load demand of 4,300 MW.

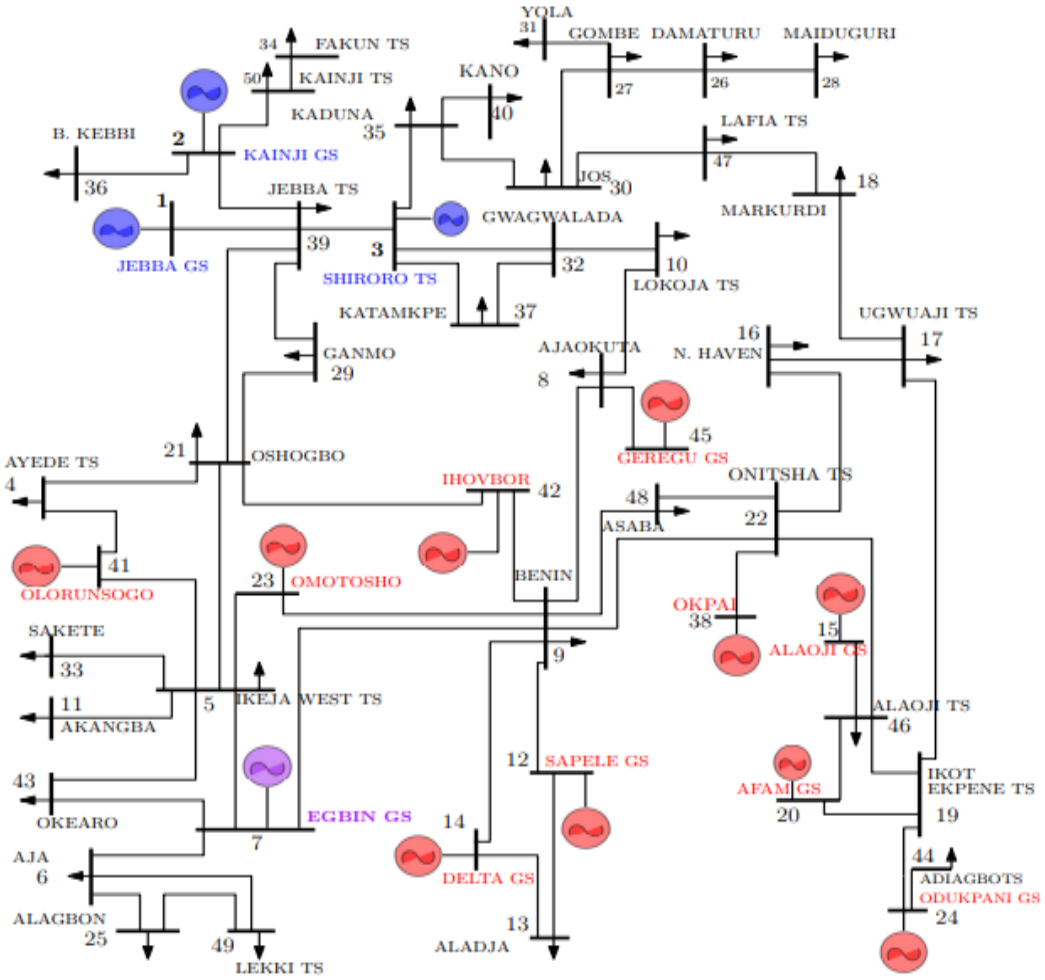

Figure 5: Single line diagram of Nigerian 50-bus power system

The Egbin power station serves as the slack bus generator, acting as the reference for both power flow analysis and voltage regulation in this investigation. The parameters used for the system's modelling were sourced from the National Control Center in Osogbo, as detailed in (Ugwuanyi *et al*., 2024b).

3.3 Renewable Energy Penetration

This study integrates RE (renewable energy) with gas-fired generators (GFGs), defining penetration as the ratio of RE output to total active power. Hydro plant outputs (Kainji, Jebba, and Shiroro) remain constant as renewable sources, while gas generation is reduced proportionally. Although hydro generation varies seasonally, it is not curtailed to prioritize RE. The slack generator and power control maintain balance.

Penetration (%) is given by

$$\text{Penetration (\%)} = \frac{P_{\text{RE}}}{P_{\text{RE}}+P_{GFG}} \times 100 \qquad (19)$$

The penetration limit is based on active power loss, though high penetration may introduce angle instability.

3.4 Case Studies

To thoroughly investigate the technical impacts of renewable energy integration, the following case studies were examined.

i. **Case 1**: This scenario represents the system without the integration of DFIG or SPV, serving as the base case. It provides a reference point to assess any improvements or deteriorations resulting from renewable energy integration. Previous studies have shown that several buses in the network experience voltage violations. To address this, STATCOM FACTS devices were strategically placed at Kano, B. Kebbi, and Gombe, as outlined in (Ugwuanyi *et al*., 2024a). Therefore, the base

case used in this study assumes the system with STATCOM already connected to correct these voltage profiles.

ii. **Case 2:** This scenario represents the system with either SPV or DFIG integrated individually into the base case.

iii. **Case 3**: This case represents the system where both SPV and DFIG are connected simultaneously.

4.0 RESULTS AND DISCUSSION

This section presents and interprets the results obtained for each of the case studies.

4.1 Analysis of Case 1

A power flow simulation was conducted on the base case to evaluate total active power loss and the voltage profile. The results indicated that seven buses—B/Kebbi, Damaturu, Gombe, Maiduguri, Jos, Yola, and Kano—had voltage levels below the 5% tolerance, ranging from 0.66 p.u. to 0.92 p.u. These voltage violations align with trends reported in NERC's 2023-2024 quarterly report, showing a strong correlation between the simulated and real-world systems. The voltage issues were resolved by integrating STATCOM FACTS devices, as outlined in Table 1.

Table 1: Base case voltage profile

Bus Name	Damaturu	Gombe	Maiduguri	Jos	Yola	Kano	B. Kebbi
Without STATCOM	0.68	0.68	0.68	0.68	0.68	0.68	0.68
With STATCOM	1.00	1.00	0.99	0.97	0.96	1.00	1.00

4.2 Analysis of Cases 2 and 3

In Case 2, a DFIG is connected to the strongest load bus (Ajah), while an SPV system is connected to Damaturu, one of the weakest buses, as identified by (Ozioko *et al*., 2022). The renewable penetration in each case is calculated using Equation (19). Load flow was rerun to determine active power loss, and the penetration limit is identified as the point of minimum loss beyond which power loss increases.

For Case 3, a DFIG (PQ-model) is connected to the strongest bus (Ajah), and an SPV system (PV-model) to a weaker bus (Damaturu bus). We selected strong buses for DFIG (PQ-model) connections to control power factor and prevent voltage profile degradation. Conversely, weak buses suit SPV (PV-model) connections, allowing voltage regulation within desirable limits. This configuration allows concurrent control of power factor and voltage using two different RE sources.

4.2.1 Impacts on active power losses

Figure 6 compares the outcomes of these cases, revealing significant improvements in penetration limits.

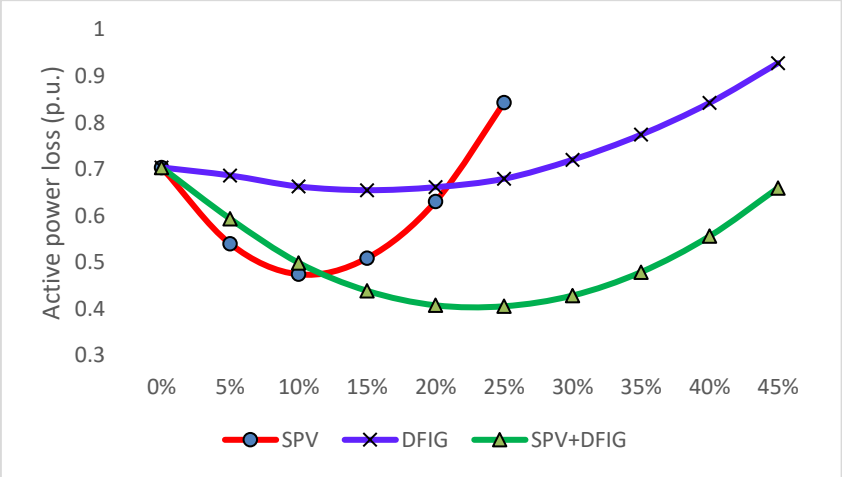

Figure 6: Active power losses versus penetration

The results show that the penetration limit for SPV alone is 10%, beyond which active power loss increases. Similarly, the penetration limit for DFIG alone is 15%. However, when SPV is combined with DFIG, the penetration limit rises to 25%. This observation suggests that carefully combining RE sources can enhance their complementarity, enabling greater renewable integration. Thus, by leveraging diverse Renewable Energy (RE) sources, the potential for substituting gas-fired generator power output with RE-based generation can be significantly expanded, enabling greater renewable integration and reduced reliance on fossil fuels. Furthermore, the combined approach drastically reduces active power losses, with additional technical advantages discussed in subsequent subsections.

4.2.2 Impacts on small-signal stability

The system's eigenvalues, along with their corresponding frequencies, damping ratios, and associated state variables for the base case, are presented in Table 2. The damping ratios and frequencies were calculated using Equations (17) and (18), respectively. It is important to note that the modes listed in this table are exclusively electromechanical modes, with a focus on those with the lowest damping. Mode 1 is moderately damped with a ratio of 6.85%, Mode 2 is poorly damped at 2.83%, and Mode 3 is reasonably damped with a ratio of 8.83%.

Table 2: The system eigenvalues for base case

Modes	Most Associated States	Eigenvalues	Damping (%)	Frequency (Hz)
1	ω_1, δ_1	-1.23878 ± j18.04234	6.85	2.88
2	ω_3, δ_3	-0.42511 ± j15.00862	2.83	2.39
3	ω_{12}, δ_{12}	-1.17622 ± j13.27573	8.83	2.12
4	ω_2, δ_2	-1.54095 ± j12.11173	12.62	1.94
5	ω_8, δ_8	-1.51342 ± j11.58388	12.95	1.86
6	ω_6, δ_6	-2.90113 ± j11.17106	25.14	1.84
7	ω_9, δ_9	-1.09453 ± j9.34384	11.63	1.50
8	ω_4, δ_4	-2.44695 ± j9.94216	23.90	1.63
9	ω_{10}, δ_{10}	-3.17551 ± j9.55715	31.53	1.60
10	ω_5, δ_5	-2.70199 ± j8.68132	29.72	1.45
11	ω_{11}, δ_{11}	-0.83006 ± j6.64272	12.40	1.07
12	ω_7, δ_7	-0.915 ± j5.12645	17.57	0.83
13	ω_{13}, δ_{13}	-0.67717 ± j4.15317	16.09	0.67

We analyzed the behavior of these three modes as the share of SPV and DFIG penetration increased, with the results displayed in Figure 7. All modes showed an increase in damping ratio up to 15% RE penetration. Beyond this point, the damping of Mode 1 and Mode 3 continued to improve. These observations suggest that the combination of SPV and DFIG enhances small-signal stability up to a 15% RE share. However, it is important to recognize that improved small-signal stability does not necessarily translate to large-signal stability, which is examined next.

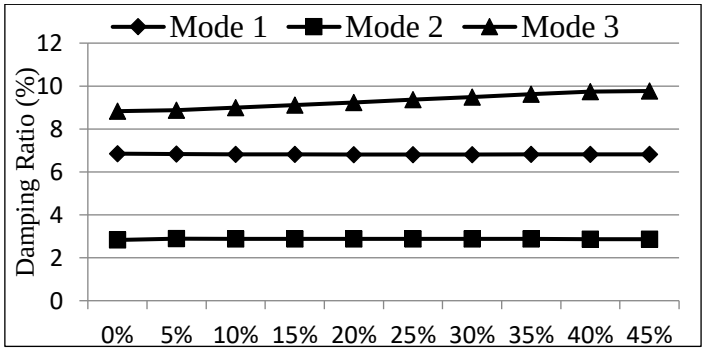

Figure 7: Damping of least damped modes vs. SPV+DFIG penetration

4.2.3 Impacts on large-signal stability

We further examined the effects of renewable energy (RE) penetration on system stability, with a specific focus on electromechanical oscillations, which are critical to power system rotor angle stability. To assess large-signal stability, we used the critical clearing time (CCT) as a key metric. A smaller CCT indicates reduced system stability, while a larger CCT suggests greater stability. The penetration limit, in this context, is defined as the maximum level of RE penetration that yields the highest CCT. Beyond this point, the CCT begins to decrease, signaling diminished stability. Electromechanical oscillations can be local or inter-area.

We simulated a fault at the Kainji bus to investigate local oscillations. As identified by (Ugwuanyi *et al*., 2021), this location is prone to nonlinear modal interactions that can compromise system stability. For each level of RE penetration, a three-phase fault was simulated at Kainji, and the corresponding CCT was calculated. Figure 8 compares the CCTs across various scenarios as RE penetration increases.

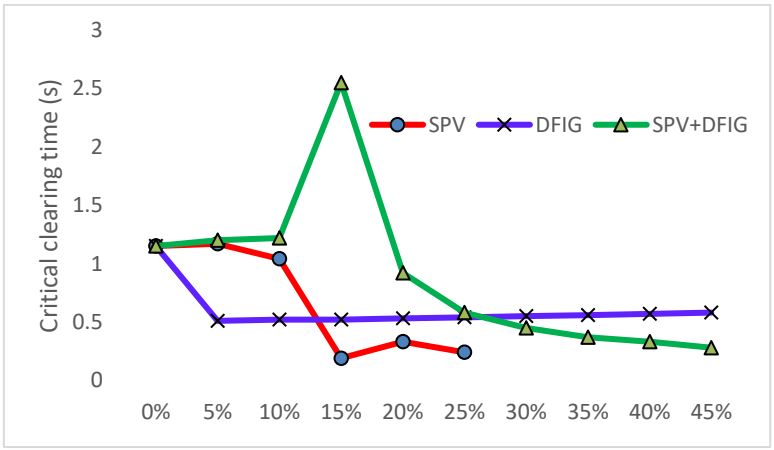

Figure 8: Critical clearing time versus RE percentage penetration for fault at Kainji

The figure illustrates that when only DFIG-based wind farm is integrated, system stability is significantly compromised, as evidenced by a CCT lower than the base case. Note that a decrease in CCT reduces the stability margin, leaving protection equipment with less time to act before cascaded instability occurs. Conversely, a higher CCT provides a larger margin for control actions, implying a more robust and resilient system. In contrast, when only SPV is employed, stability improves up to a 5% integration level, after which the CCT begins to decline. However, when both SPV and DFIG are integrated simultaneously, system stability is notably enhanced, allowing up to 15% RE penetration. At this penetration level, the CCT reaches approximately 2.5 seconds, compared to the base case value of 1.15 seconds—representing a 117% improvement in the stability of local oscillations. Although this improvement is substantial, inter-area oscillations remain the most critical concern in power systems, as they involve multiple generators across the network and pose a greater challenge to overall system stability. Thus, we investigated the inter-area oscillation with results shown in Figure 9.

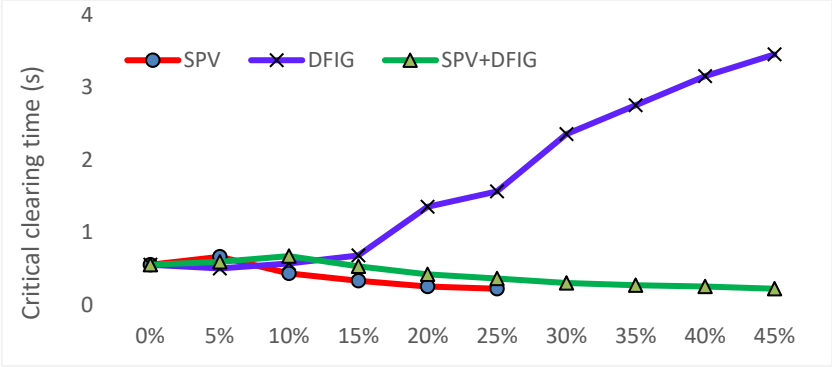

Figure 9: Critical clearing time versus RE percentage penetration for fault at Ihovbor

As noted by (Ugwuanyi *et al*., 2021), a fault at the Ihovbor generator can trigger inter-area oscillations. To study this, we simulated a three-phase fault, similar to the approach used for local oscillations. From the results, it is evident that with SPV alone, system stability is maintained up to a 5% penetration limit, as the CCT decreases beyond this point. With DFIG alone, the CCT starts to improve only from 15% RE penetration and continues indefinitely. However, this is not considered a gain since beyond this 15% threshold, active power losses begin to increase, as shown in Figure 6. When both SPV and DFIG are integrated, the CCT increases up to 10% RE penetration, after which it starts to decline. At 10% penetration, the CCT reaches 0.67 seconds, higher than the base case value of 0.55 seconds—representing a 22% improvement in inter-area oscillation stability. This 22% improvement is significant, given the severity of inter-area oscillations, which involve multiple generators and are more challenging to stabilize. These findings indicate that combining RE sources like SPV and DFIG can improve both small- and large-signal stability. This mix is especially beneficial in areas with abundant RE potential, enhancing system stability and mitigating the risks associated with high RE penetration levels.

4.0 CONCLUSION

The study offers a comprehensive technical analysis of integrating solar and wind energy into Nigeria's 330 kV grid, focusing on their impact on stability and active power loss. The results show that integrating solar photovoltaic (SPV) and doubly-fed induction generator (DFIG) wind systems provides significant benefits in terms of grid stability and reduced power losses. The study found that SPV and DFIG complement each other, allowing for a combined renewable energy penetration of up to 25%, leading to reduced active power losses and improved small- and large-signal stability. In small-signal stability analysis, the damping ratios of critical electromechanical modes improved as renewable energy penetration increased, particularly up to 15%. For large-signal stability, the combination of SPV and DFIG also improved the system's critical clearing time (CCT), enhancing stability under fault conditions, particularly in scenarios involving local oscillations. While inter-area oscillations remain a challenge, the combined integration of wind and solar energy demonstrated a 22% improvement in inter-area oscillation stability. In conclusion, the study suggests that the concurrent use of SPV and DFIG can significantly enhance grid performance and stability, making renewable energy integration a viable strategy for reducing Nigeria's reliance on fossil fuels while addressing key stability challenges in its power grid. The findings underscore the importance of careful planning and optimal placement of renewable sources to maximize the benefits of hybrid renewable systems in areas with high renewable energy potential.

REFERENCES

Adedipe, O., Abolarin, M. S. and Mamman, R. O. (2018). A Review of Onshore and Offshore Wind Energy Potential in Nigeria. *2018 IOP Conference Series: Materials Science and Engineering*, Vol. 413, pp. 1-8.

Adetokun, B. B., Muriithi, C. M. and Ojo, J. O. (2020). Voltage Stability Assessment and Enhancement of Power Grid with Increasing Wind Energy Penetration. *International Journal of Electrical Power & Energy Systems*, Vol. 120, pp. 1-14.

Adetokun, B. B., Ojo, J. O. and Muriithi, C. C. (2021). Application of Large-Scale Grid-Connected Solar Photovoltaic System for Voltage Stability Improvement of Weak National Grids. *Scientific Reports*, Vol. 11, No. 1, pp. 1-16.

Akuru, U. B., Onukwube, I. E., Okoro, O. I. and Obe, E. S. (2017). Towards 100% Renewable Energy in Nigeria. *Renewable and Sustainable Energy Reviews*, Vol. 71, pp. 943-953.

Anichebe, I. B. and Ekwue, A. O. (2020). Improvement of Bus Voltage Profiles of Nigerian Power Network in the Presence of Static Synchronous Compensator (STATCOM) and Doubly Fed Induction Generator (DFIG). *Nigerian Journal of Technology (NIJOTECH)*, Vol. 39, No. 1, pp. 228-237.

Atta, H., Kamarposhti, M. A. and Solyman, A. A. A. (2022). Impacts of Integration of wind Farms on Voltage Stability Margin. *International Journal of Electrical and Computer Engineering (IJECE)*, Vol. 12, No. 5, pp. 4623-4631.

Ayodele, T. R., Jimoh, A. A., Munda, J. L. and Agee, J. T. (2013). The Influence of Wind Power on the Small Signal Stability of a Power System. *RE & PQJ*, Vol. 1, No. 9, pp. 244-249.

Bekri, O. E. F. I. and Mekri, F. (2018). Impact of Wind Turbine on Voltage Stability, *2018 International Conference on Wind Energy and Applications in Algeria (ICWEAA)*, Algiers, Algeria, 6-7 November, 2018, pp. 1-5.

Berrutti, F., Giusto, A. and Artenstein, M. (2012). Modal Analysis of the Uruguayan Power System Incorporating Large Scale Wind Generation. *2012 Sixth IEEE/PES Transmission and Distribution: Latin America Conference and Exposition (T&D-LA)*, Montevideo, Uruguay, 3-5 September, 2012, pp. 1-6.

Brown, T. W., Bischof-Niemz, T., Blok, K., Breyer, C., Lund, H. and Mathiesen, B. V. (2018). Response to 'Burden of Proof: A Comprehensive Review of the Feasibility of 100% Renewable-Electricity Systems'. *Renewable and Sustainable Energy Reviews*, Vol. 92, pp. 834-847.

Chau, T. K. (2019). Small Signal Stability Analysis and Wide Area Damping for Complex Power System Integrated with Renewable Energy Sources. *Thesis for Doctor of Philosophy*, University of West Australia.

Chukwulobe, O. O., Obi, P. I., Amako, E. A. and Ezeonye, C. S. (2022). Improved Under-Voltage Load Shedding Scheme in Power System Network for South Eastern Nigeria. *NIPES Journal of Science and Technology Research*, Vol. 4, No. 1, pp. 212-223.

Dhouib, B., Alaas, Z., Kahouli, O. and Abdallah, H. H. (2020). Determination of Optimal Location of FACTS Device to Improve Integration Rate of Wind Energy in Presence of MBPSS Regulator. *The Institution of Engineering and Technology*, Vol. 14, No. 17, pp. 3526-3540.

Emeasoba, A. B., Ezeonye, C. S. and Obi, P. I. (2023). Optimal Fuel Cost of Power Generation in Nigeria: A Case Study of Omoku Power Station. *International Journal of Innovative Engineering, Technology & Science*, Vol. 7, No. 1, pp. 64-76.

Emeghara, M. C., Obi, P. I. and Onah, A. J. (2022). Modeling and Performance Evaluation of a Hybrid Solar-Wind Power Generation Plant. *Journal of Energy Technology and Environment*, Vol. 4, No. 1, pp. 21-37.

Essallah, S., Bouallegue, A. and Khedher A. (2019). Integration of Automatic Voltage Regulator and Power System Stabilizer: Small-Signal Stability in DFIG-Based Wind Farms, *J. Mod. Power Syst. Clean Energy*, Vol. 7, No. 1-14.

Feijoo, A. E. and Cidras, J. (2000). Modeling of Wind Farms in the Load Flow Analysis. *IEEE Transactions on Power Systems*, Vol. 15, No. 1, pp. 110-115.

Gurung, N., Bhattarai, R. and Kamalasadan, S. (2020). Optimal Oscillation Damping Controller Design for Large-Scale Wind Integrated Power Grid. *IEEE Transaction on Industry Applications*, Vol. 56, No. 4, pp. 4225-4235.

Krismanto, A. U., Sulistiawati, I. B., Limpraptono, F. Y., Priyad, A., Setiadi, H. and Abdillah, M. (2021). Impact of Large-Scale Wind Power Penetration on Dynamic Voltage Stability of Interconnected Power System: An Indonesia Case Study. *International Journal of Intelligent Engineering and Systems*, Vol. 14, No. 4, pp. 251-263.

Mas'ud, A. A., Wirba, A. V., Muhammad-Sukki, F., Mas'ud, I. B., Munir, A. B. and Yunus, N. M. (2015). An Assessment of Renewable Energy Readiness in Africa: A Case Study of Nigeria and Cameroon. *Renewable and Sustainable Energy Reviews*, Vol. 51, pp. 775-784.

Mohammed, Y. S., Mustafa, M. W., Bashir, N. and Ibrahem, I. S. (2017). Existing and Recommended Renewable and Sustainable Energy Development in Nigeria Based on Autonomous Energy and Microgrid Technologies. *Renewable and Sustainable Energy Reviews*, Vol. 75, pp. 820-838.

Narayanan, A., Mets, K., Strobbe, M. and Develder, C. (2019). Feasibility of 100% Renewable Energy Based Electricity Production for Cities with Storage and Flexibility. *Renewable Energy*, Vol. 134, pp. 698-709.

Naser, I. S., Alsharif, M., Rafa, A. H. and Ahmed, A. A. (2021). Impact of Wind Farm Location on Voltage Stability. *Journal of Pure & Applied Science*, Vol. 20, No. 4, pp. 198-201.

Nkan, I. E., Okoro, O. I., Obi, P. I., Awah, C. C. and Akuru, U. B. (2019). Application of FACTS Devices in a Multi-Machine Power System Network for Transient Stability Enhancement: A Case Study of the Nigerian 330 kV 48-Bus System. *2019 IEEE AFRICON*, Accra, Ghana, 25-27 September, 2019, pp. 1-9.

Obi, P. I., Amako, E. A. and Ezeonye, C. S. (2022). Comparative Financial Evaluation of Technical Losses in South Eastern Nigeria Power Network. *Bayero Journal of Engineering and Technology (BJET)*, Vol. 17, No. 2, pp. 41-51.

Obi, P. I., Ezeonye, C. S. and Amako, E. A. (2021). Appropriate Energy Mix to Facilitate Rural Industrial Development and Economic Growth in Nigeria. *Proceedings of 3rd International Conference on Research and Innovations in Engineering*, Uyo, Nigeria, 20-24 September, 2021, pp. 13-28.

Offiong, N. S., Kalu, C. and Nseobong, O. (2022). Comparative Evaluation of SSSC and STATCOM FACTS Devices Power Transfer Capability Enhancement on the Nigerian 330 kV Power Network. *International Multilingual Journal of Science and Technology*, Vol. 7, No. 8, pp. 6074-6086.

Ogunbiyi, O., Adesina, L. M., Ugwute, F. O. and Thomas, C. T. (2022). Enhancement of the Nigerian National Grid Performance with a FACT Compensator. *Nigerian Research Journal of Engineering and Environmental Sciences*, Vol. 7, No. 2, pp. 506-518.

Ohunakin, O. S., Adaramola, M. S., Oyewola, O. M. and Fagbenle, R. O. (2014). Solar Energy Applications and Development in Nigeria: Drivers and Barriers. *Renewable and Sustainable Energy Reviews*, Vol. 32, pp. 294-301.

Okedu, K. E., Oyinna, B., Colak, I. and Kalam, A. (2024). Geographical Information System Based Assessment of Various Renewable Energy Potentials in Nigeria. *Energy Reports*, Vol. 11, pp. 1147-1160.

Okeniyi, J. O., Ohunakin, O. S. and Okeniyi, E. T. (2015). Assessment of Wind Energy Potentials in Three Selected Locations in Nigeria: Implication for Renewable/Sustainable Rural Electrification. *Scientific World Journal*, Vol. 2015, pp. 1-13.

Olanrewaju, A. O., Nwohu, M. N., Adegboye, B. A. and Omojhafe, J. T. (2022). Integration of Wind Power into Nigerian 330 kV Grid Network for Voltage Stability and Loadability Enhancement. *SSRN Preprint*, pp. 1-22.

Oluleye, A. and Debo, A. (2016). Wind Energy Density in Nigeria as Estimated from the ERA Interim Reanalysed Data Set. *Current Journal of Applied Science and Technology*, Vol. 17, No. 1, pp. 1-17.

Ozioko, I. O., Ugwuanyi, N. S., Ekwue, A. O. and Odeh, C. I. (2022). Wind Energy Penetration Impact on Active Power Flow in Developing Grid. *Scientific African*, Vol. 18, pp. 14-22.

Qin, B., Li, H., Zhang, X., Ding, T., Ma, K. and Mei, S. (2020). Quantitative Short-Term Voltage Stability Analysis of Power Systems Integrated with DFIG-Based Wind Farms. *IET Generation, Transmission & Distribution*, Vol. 14, No. 19, pp. 4264-4272.

REN21 (2020). Renewables Global Status Report (GSR 2020). https://www.ren21.net/wp-content/uploads/2019/05/gsr_2020_full_report_en. Accessed on 20/08/2023.

Sambo, A. (2009). Strategic Developments in Renewable Energy in Nigeria. *International Association for Energy Economics*, Vol. 1, pp. 15-19.

Shaaban, M. and Petinrin, J. O. (2014). Renewable Energy Potentials in Nigeria: Meeting Rural Energy Needs. *Renewable and Sustainable Energy Reviews*, Vol. 29, pp. 72-84.

Somoye, O. A. (2023). Energy Crisis and Renewable Energy Potentials in Nigeria: A Review. *Renewable and Sustainable Energy Reviews*, Vol. 188, pp. 1-13.

Srivastava, A., Meena, R. and Parida, S. K. (2018). Effect of PV and FACTS on Small Signal Stability. *Proceedings of the National Power Systems Conference (NPSC)*, NIT Tiruchirappalli, India, 14-16 December, 2018, pp. 1-5.

Tavakoli, S. D., Prieto-Araujo, E., Sánchez-Sánchez, E. and Gomis-Bellmunt, O. (2020). Interaction Assessment and Stability Analysis of the MMC-Based VSC-HVDC Link. *Energies*, Vol. 13, No. 8, pp. 1-19.

Ugwuanyi, N. S., Nwogu, O. A., Ozioko, I. O., and Ekwue, A. O. (2024). An Easy Method for Simultaneously Enhancing Power System Voltage and Angle Stability using STATCOM. *Scientific African*, Vol 25, pp. 1-9.

Ugwuanyi, N. S., Ozioko, I. O. and Ugwuoke, N. C. (2024). Dataset for the Nigerian 50-Bus 330 kV Power Grid. *Zenodo*, pp. 1-7. https://dx.doi.org/10.5281/zenodo.12091189. Accessed on 20/08/2023.

Ugwuanyi, N. S., Ozioko, I. O., Uma, U. U., Nwogu, O. A., Ugwuoke, N. C., Ekwue, A. O. and Nwokocha, N. (2024). Enhancing Renewable Energy-Grid Integration by Optimally Placed FACTS Devices: The Nigeria Case Study. *Science Journal of Energy Engineering*, Vol. 12, No. 2, pp. 16-25.

Ugwuanyi, N. S., Uma, U. U. and Ekwue, A. O. (2021). Fundamental Study of Oscillations in the Nigerian Power System. *Nigerian Journal of Technology (NIJOTECH)*, Vol. 40, No. 5, pp. 913-926.

Ukoima, K. N., Obi, P. I. and Ezeonye, C. S. (2019). Dynamic Modelling of Excitation and Governor Effect on Stability of Electrical Machines. *2nd International Engineering Conference, IECON 2019*, Umudike, Nigeria,2-4 September, 2019, pp. 1-11.

Yang, M., Li, Y., Wen, J., Liu, C., Zhu, M. and Liang, T. (2013). A Study on Small Signal Stability of the Large-Scale Wind Farm with DFIGs. *Advanced Materials Research*, Vol. 765-767, pp. 2579-2585.

Zappa, W., Junginger, M. and Van Den Broek, M. (2019). Is a 100% Renewable European Power System Feasible by 2050. *Applied Energy*, Vol. 233–234, pp. 1027-1050.